Chinese Chemical Letters 33 (2022) 4559–4562

Contents lists available at ScienceDirect

Chinese Chemical Letters

journal homepage: www.elsevier.com/locate/cclet

Porphyrin covalent organic framework for photocatalytic synthesis of tetrahydroquinolines

Chengjuan Wu[1], Xinyu Li[1], Mingzhen Shao, Jinglan Kan, Guangbo Wang, Yan Geng*, Yu-Bin Dong*

College of Chemistry, Chemical Engineering and Materials Science, Collaborative Innovation Center of Functionalized Probes for Chemical Imaging in Universities of Shandong, Key Laboratory of Molecular and Nano Probes, Ministry of Education, Shandong Normal University, Ji'nan 250014, China

ARTICLE INFO

Article history:
Received 29 October 2021
Revised 21 January 2022
Accepted 24 January 2022
Available online 31 January 2022

Keywords:
Tetrahydroquinolines
Photocatalytic oxidative annulation
Covalent organic framework
Heterogeneous photocatalyst
Porphyrin

ABSTRACT

A metal-free porphyrin covalent organic framework was employed as the heterogeneous photocatalyst for the synthesis of tetrahydroquinolines under aerobic conditions. With visible light irradiation of a catalytic amount of H_2P-Bph-COF at room temperature, various substituted *N*,*N*-dimethylanilines and *N*-aryl maleimides were transformed to tetrahydroquinoline derivatives in moderate to good yields. This was the first example of the synthesis of tetrahydroquinolines *via* the photocatalytic aerobic annulation reaction employing the metal-free COF as the heterogeneous photocatalyst.

Tetrahydroquinolines and their derivatives are important scaffolds which are widely found in natural products and synthetic drugs [1–4]. Various methods have been developed for the synthesis of tetrahydroquinoline skeletons thus far [5,6]. Among them, the oxidative annulation of *N*,*N*-dimethylaniline with maleimide holds special interest, which provides a convenient and efficient protocol to access tetrahydroquinolines [7–12]. As is shown, this reported oxidative annulation strategy usually involves the metal catalysts together with molecular oxygen or organic oxidants. Despite the remarkable success, this approach, however, generally requires harsh reaction conditions in most cases. Photocatalysis is considered as an eco-friendly and powerful synthetic technique, which can promote functional-group transformations with the photon as a green source of energy and a traceless reagent [13–21]. It provides a competitive alternative to tetrahydroquinolines synthesis [22–33], in which a variety of photoactive molecular metal complexes and organic dyes, including $Ru(bpy)_3Cl_2$, $Ir(ppy)_2(dtbbpy)PF_6$, $[Cu(dap)_2]Cl$ and Eosin Y, have been employed as the photocatalysts. However, these photocatalysts are usually homogeneous, which would lead to the difficult catalyst separation and recovery. Therefore, the design and synthesis of recyclable and efficient heterogeneous photocatalysts for the photocatalytic aerobic annulation reactions are of great importance.

Covalent organic frameworks (COFs), as an emerging class of organic crystalline porous materials with highly ordered and extended structures, have recently received increasing attention [34]. Due to their tuneability, high chemical stability, and excellent optical properties, COFs are found to be efficient heterogeneous photocatalysts for a series of organic transformations [35–48]. However, the COF-based photocatalytic aerobic annulation to tetrahydroquinolines has been rarely reported. Very recently, a Pt-metallated COF was reported to serve as the photocatalyst for oxidative annulation, in which the loaded Pt enhanced the photocatalytic activity of COF [49]. To meet the requirements of resource-saving and low-cost aerobic annulation, we envisioned that the metal-free porphyrin [50–52] COF with unique photophysical and photochemical properties could be the efficient photocatalyst for such transformation.

Herein, we report, for the first time, a metal-free porphyrin COF (H_2P-Bph-COF)-based protocol for the synthesis of tetrahydroquinolines *via* photocatalytic aerobic annulation. In the presence of H_2P-Bph-COF, various tetrahydroquinolines were obtained by the combination of *N*,*N*-dimethylanilines with maleimides under visible-light irradiation at room temperature. Furthermore, the obtained H_2P-Bph-COF heterogeneous photocatalyst was robust,

* Corresponding authors.
E-mail addresses: gengyan@sdnu.edu.cn (Y. Geng), yubindong@sdnu.edu.cn (Y.-B. Dong).
[1] These authors contributed equally to this work.

https://doi.org/10.1016/j.cclet.2022.01.065
1001-8417/

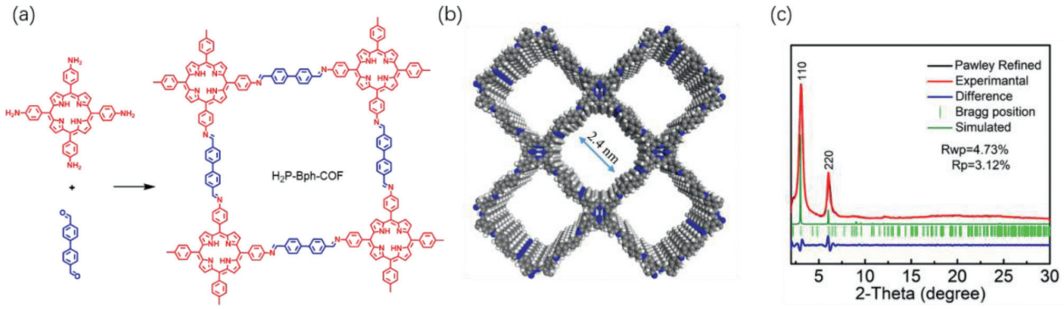

Fig. 1. (a) Schematic representation of the synthesis of H_2P-Bph-COF (HOAc, *o*-dichlorobenzene/*n*-BuOH, 120 °C, 3 days). (b) Top view of the eclipsed structure proposed for H_2P-Bph-COF (gray, C; blue, N; and white, H). (c) Indexed experimental (red), Pawley-refined (black), and simulated (green) PXRD patterns of H_2P-Bph-COF. The difference plot is presented in blue.

and could be reused at least five times without loss in its catalytic activity. To the best of our knowledge, the photocatalytic aerobic annulation reaction employing the metal-free COF as the heterogeneous photocatalyst has not been reported thus far.

As shown in Fig. 1a, the porphyrin COF of H_2P-Bph-COF was synthesized by the acid-catalyzed Schiff-base condensation between 5,10,15,20-tetra(*p*-amino-phenyl)porphyrin (H_2TAPP) and 4,4′-biphenyldialdehyde under solvothermal conditions (HOAc, *o*-dichlorobenzene/*n*-BuOH, 120 °C, 3 days). H_2P-Bph-COF was obtained as the purple crystalline solids [53,54]. The formation of H_2P-Bph-COF was confirmed by Fourier transform infrared (FT-IR). The peaks of 1695 cm^{-1} for C=O and 3338 cm^{-1} for N-H were strongly attenuated, while a new characteristic C=N stretching vibration band at 1626 cm^{-1} was observed in the FT-IR spectrum of H_2P-Bph-COF, implying the formation of the imine bond (Fig. S1 in Supporting information). Powder X-ray diffraction (PXRD) analysis indicated the good crystallinity of the obtained H_2P-Bph-COF. As shown in Fig. 1c, the PXRD diagram of H_2P-Bph-COF exhibited two intense peaks at 3.09° and 6.04°, which were attributed to (110) and (220) planes, respectively. The simulation of its PXRD pattern with Materials Studio (version 2018) suggested that H_2P-Bph-COF possessed the 2D network with eclipsed AA-type stacking mode. The Pawley refinement indicated a negligible difference between the simulated and experimental PXRD patterns. H_2P-Bph-COF was assigned to the space group *P*4 with optimized parameters of $a = b = 41.49$ Å, $c = 3.67$ Å, $\alpha = \beta = \gamma = 90°$, residuals $R_{wp} = 4.73\%$ and $R_p = 3.12\%$.

The porosity of H_2P-Bph-COF was investigated by N_2 adsorption-desorption measurements at 77 K (Fig. S2 in Supporting information). The Brunauer-Emmett-Teller (BET) surface area of H_2P-Bph-COF was determined as 413 m^2/g, and the total pore volume was calculated to be 0.32 cm^3/g. The pore size distribution was mainly centered at *ca.* 2.0 nm based on nonlocal density functional theory (NLDFT) (Fig. S3 in Supporting information). The morphology of H_2P-Bph-COF was examined by scanning electron microscopy (SEM), which showed that the obtained H_2P-Bph-COF features micrometer-scale lamellar morphology (Fig. S4 in Supporting information). Thermogravimetric analysis (TGA) indicated that H_2P-Bph-COF remains stable up to *ca.* 240 °C, suggesting its good thermal stability (Fig. S5 in Supporting information).

We initially choose *N*,*N*-dimethylaniline (**1a**) and *N*-phenylmaleimide (**2a**) as the model substrates to carry out the photocatalytic oxidative annulation reaction. When the mixture, containing the substrates and a catalytic amount of H_2P-Bph-COF (8 mol%) as the photocatalyst in DMF, was irradiated by blue LEDs ($\lambda = 450$ nm) under an oxygen atmosphere for 12 h, the desired annulated product of **3a** was obtained in 50% yield (Table 1, entry 1). Screening of the solvents showed that $CHCl_3$ was the best to give the product in 71% yield, while only a trace amount of annulated

Table 1
Optimization of the H_2P-Bph-COF catalyzed photocatalytic aerobic annulation reaction conditions.[a]

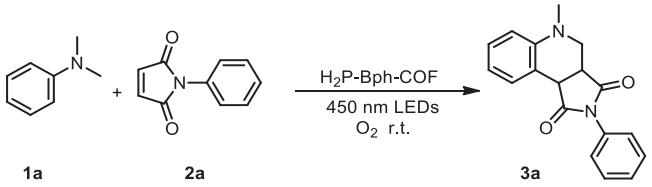

1a 2a 3a

Entry	H_2P-Bph-COF (mol%)	Solvent	Time (h)	Yield[b] (%)
1	8	DMF	12	50
2	8	Acetone	12	56
3	8	CH_3CN	12	49
4	8	CH_3OH	12	trace
5	8	THF	12	trace
6	8	$CHCl_3$	12	71
7	6	$CHCl_3$	12	66
8	10	$CHCl_3$	12	71
9	8	$CHCl_3$	14	76 (72)[c]
10	8	$CHCl_3$	16	76
11[d]	8	$CHCl_3$	16	35
12[e]	8	$CHCl_3$	14	N.R.
13	–	$CHCl_3$	14	N.R.

[a] Reaction conditions: 0.2 mmol **1a**, 0.1 mmol **2a**, corresponding H_2P-Bph-COF were added in 3 mL solvent, and the solution was irradiated under blue LEDs ($\lambda = 450$ nm) at room temperature in oxygen.
[b] Yield was determined by ^{1}H NMR analysis of the reaction mixture using mesitylene as an internal standard.
[c] The isolated yield is given in parentheses.
[d] In air.
[e] In dark.

product was detected in MeOH or THF under the given conditions (Table 1, entries 2–6). On the other hand, the less catalyst loading (6 mol%) resulted in a lower 66% yield (Table 1, entry 7), while the more catalyst loading of 10 mol% did not lead to higher yield (Table 1, entry 8). In addition, the longer reaction time of 14 h and 16 h caused a slightly higher 76% yield for **3a** (Table 1, entries 9 and 10). Further assessment revealed that the oxygen atmosphere is necessary (Table 1, entry 11). Control experiments indicated that both H_2P-Bph-COF and visible-light were essential for this aerobic annulation reaction (Table 1, entries 12 and 13). As such, the optimized conditions for synthesis of tetrahydroquinoline are as follows: 0.2 mmol **1a**, 0.1 mmol **2a**, and 8 mol% H_2P-Bph-COF in 3 mL $CHCl_3$, irradiated by blue LEDs under an oxygen atmosphere for 14 h at room temperature.

The leaching test demonstrated that H_2P-Bph-COF was a typical heterogeneous catalyst (Fig. S6 in Supporting information), and the yield of the annulation product **3a** was still up to 73% after five catalytic runs (Fig. S7 in Supporting information). The measured PXRD pattern of H_2P-Bph-COF was intact after five catalytic runs,

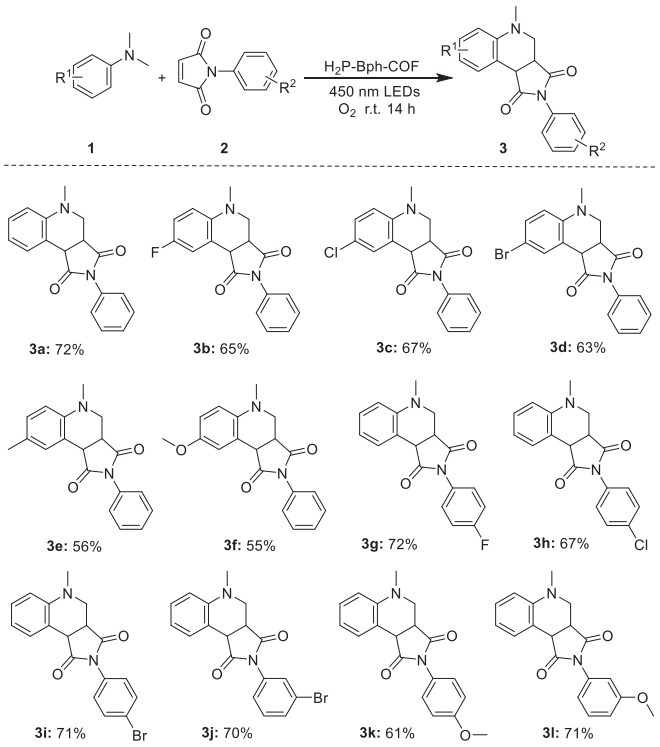

Scheme 1. Scope of the H_2P-Bph-COF catalyzed photocatalytic aerobic annulation reaction. Reaction conditions: **1** (0.2 mmol), **2** (0.1 mmol), 8 mol% H_2P-Bph-COF, 3 mL $CHCl_3$, blue LEDs ($\lambda = 450$ nm), 14 h, room temperature, in oxygen. Isolated yields are shown.

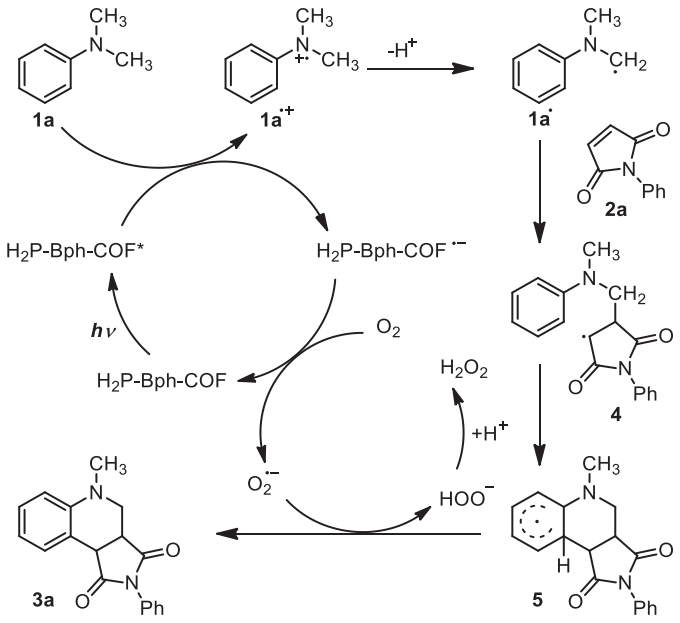

Scheme 2. Proposed reaction mechanism.

implying that its excellent stability and recyclability of H_2P-Bph-COF in photocatalysis (Fig. S8 in Supporting information).

With the optimal reaction condition in hand, we explored the generality of this aerobic reaction. As shown in Scheme 1, a variety of *N,N*-dimethylanilines with electron-donating or electron-withdrawing groups could smoothly react with *N*-phenylmaleimide (**2a**) under the optimized reaction conditions, affording the desired annulated products in moderate-to-good yields (**3b**-**3f**). Furthermore, the scope of *N*-phenylmaleimide was also examined. When the *N,N*-dimethylaniline (**1a**) reacted with electronically diverse *N*-aryl maleimides bearing halogens (**3g-3j**) and alkoxy (**3k-3l**) groups at the *meta*-, and *para*- positions of aryl ring, the corresponding tetrahydroquinolines were generated in moderate-to-good yields. We have also investigated the scope of *N*-alkyl maleimides. *N*-Benzyl maleimide could react with *N,N*-dimethylaniline to afford the desired product in 32% yield (**3m**). Only a trace amount of annulated product (**3n**) was detected for the reaction of *N*-methyl maleimide with *N,N*-dimethylaniline (Scheme S3 in Supporting information).

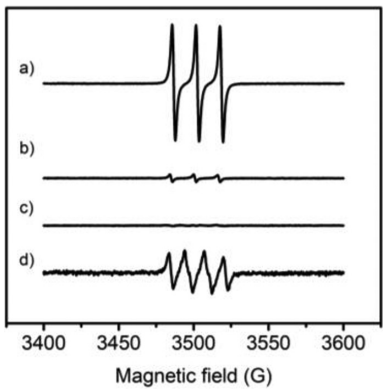

Fig. 2. ESR measurements of (a) $CHCl_3$ solution of H_2P-Bph-COF and TEMP irradiated by blue LEDs; (b) $CHCl_3$ solution of H_2P-Bph-COF, **1a** and TEMP irradiated by blue LEDs; (c) $CHCl_3$ solution of H_2P-Bph-COF and DMPO irradiated by blue LEDs; (d) $CHCl_3$ solution of H_2P-Bph-COF, **1a** and DMPO irradiated by blue LEDs.

To understand the reaction process of the system, cyclic voltammetry of H_2P-Bph-COF was performed. As is shown in Fig. S9 (Supporting information), an onset potential at −0.80 V *vs.* Fc/Fc^+, attributable to the redox potential of $E_{H_2P\text{-Bph-COF}/H_2P\text{-Bph-COF}^{\bullet-}}$ was observed. In addition, the UV–vis diffuse reflectance spectrum of H_2P-Bph-COF displayed a broad absorption up to *ca.* 660 nm, and the optical band gap (E_g) was calculated to be 1.75 eV according to the Tauc plots (Fig. S10 in Supporting information). Thus, the reduction potential of $E_{H_2P\text{-Bph-COF}^*/H_2P\text{-Bph-COF}^{\bullet-}}$ was determined to be 0.95 V *vs.* Fc/Fc^+ [55–58]. On the other hand, the oxidation potential of **1a** ($E_{\mathbf{1a}^{\bullet+}/\mathbf{1a}}$) was known as 0.34 V *vs.* Fc/Fc^+ [59,60]. These results proved the thermodynamic feasibility of the photoinduced electron transfer from **1a** to H_2P-Bph-COF*.

In order to determine the function of molecular oxygen, we performed the electron-spin resonance (ESR) measurement to study the reactive oxygen species (ROS) generated in the system. Thereinto, 2,2,6,6-tetramethylpiperidine (TEMP) was employed as a probe to trap $^1O_2$, and 5,5-dimethyl-1-pyrroline-*N*-oxide (DMPO) was used to capture $O_2^{\bullet-}$. As shown in Fig. 2, the characteristic signal of $^1O_2$ was observed when the system containing H_2P-Bph-COF and TEMP was irradiated by blue LEDs, and the $^1O_2$ signal was strongly attenuated after the addition of **1a**. In contrast, no signal was detected in the system containing DMPO and H_2P-Bph-COF irradiated by blue LEDs. However, the characteristic signal of $O_2^{\bullet-}$ captured by DMPO was clearly observed after the addition of **1a**, indicating the formation of $O_2^{\bullet-}$, a crucial species for the oxidative annulation reaction, *via* a photoinduced electron transfer process.

Based on above results and previous reports [22–33], we proposed the reaction mechanism for this transformation. As shown in Scheme 2, upon irradiation by visible-light, the H_2P-Bph-COF was activated to its excited state H_2P-Bph-COF*. The electron transfer from **1a** to H_2P-Bph-COF* led to the formation of $\mathbf{1a}^{\bullet+}$ and H_2P-Bph-$COF^{\bullet-}$. The generated H_2P-Bph-$COF^{\bullet-}$ further reacted with O_2 to produce $O_2^{\bullet-}$, accompanying the regeneration of H_2P-Bph-COF. Meanwhile, the generated $\mathbf{1a}^{\bullet+}$ further lose one proton to afford α-aminoalkyl radical $\mathbf{1a}^{\bullet}$, which followed to react with **2a** to pro-

duce radical **4**. Subsequently, the generated **4** underwent cyclization to form intermediate **5**. Finally, the oxidation and deprotonation of intermediate **5** assisted by $O_2^{\bullet-}$ afforded the desired product **3a**, with the formation of H_2O_2.

In summary, we report a metal-free porphyrin COF and its application in photocatalytic oxidative annulation reaction of *N*,*N*-dimethylanilines with maleimides. Upon visible-light irradiation, the metal-free H_2P-Bph-COF can be a highly efficient heterogeneous and reusable photocatalyst to promote the formation of various substituted tetrahydroquinolines in moderate to good yields under mild conditions. We believe that the photoactive COF-based synthetic protocol herein not only provides a green and facile way to access tetrahydroquinolines synthesis, but also significantly expands the application scope of COF-based catalysts.

Declaration of competing interest

The authors declare that they have no known competing financial interests or personal relationships that could have appeared to influence the work reported in this paper.

Acknowledgments

We are grateful for the financial support from the National Natural Science Foundation of China (Nos. 22101158, 22171169, 21971153 and 21772116), the Natural Science Foundation of Shandong Province (No. ZR2021MB088), the Taishan Scholars Climbing Program of Shandong Province, the Taishan Scholar Project of Shandong Province, and the Major Basic Research Projects of Shandong Natural Science Foundation (No. ZR2020ZD32).

Supplementary materials

Supplementary material associated with this article can be found, in the online version, at doi:10.1016/j.cclet.2022.01.065.

References

[1] A. Cappelli, C. Nannicini, S. Valenti, et al., ChemMedChem 5 (2010) 739–748.
[2] K. Grychowska, G. Satała, T. Kos, et al., ACS Chem. Neurosci. 7 (2016) 972–983.
[3] J.P. Michael, Nat. Prod. Rep. 20 (2003) 476–493.
[4] D.V. Kravchenko, Y.A. Kuzovkova, V.M. Kysil, et al., J. Med. Chem. 48 (2005) 3680–3683.
[5] B. Nammalwar, R.A. Bunce, Molecules 19 (2014) 204–232.
[6] I. Muthukrishnan, V. Sridharan, J.C. Menéndez, Chem. Rev. 119 (2019) 5057–5191.
[7] M. Nishino, K. Hirano, T. Satoh, M. Miura, J. Org. Chem. 76 (2011) 6447–6451.
[8] N. Sakai, S. Matsumoto, Y. Ogiwara, Tetrahedron Lett. 57 (2016) 5449–5452.
[9] Z. Song, A.P. Antonchick, Tetrahedron 72 (2016) 7715–7721.
[10] A.K. Yadav, L.D.S. Yadav, Tetrahedron Lett. 57 (2016) 1489–1491.
[11] K. Sharma, B. Das, P. Gogoi, New J. Chem. 42 (2018) 18894–18905.
[12] J.Y. Hwang, A.Y. Ji, S.H. Lee, E.J. Kang, Org. Lett. 22 (2020) 16–21.
[13] Q.W. Gui, F. Teng, Z.C. Li, et al., Chin. Chem. Lett. 32 (2021) 1907–1910.
[14] W.B. He, L.Q. Gao, X.J. Chen, et al., Chin. Chem. Lett. 31 (2020) 1895–1898.
[15] K. Sun, F. Xiao, B. Yu, W.M. He, Chin. J. Catal. 42 (2021) 1921–1943.
[16] C. Hou, H. Liu, F.B. Mohammad, J. Solid State Chem. 300 (2021) 122288.
[17] C. Hou, H. Liu, Y. Li, RSC Adv. 11 (2021) 14957–14969.
[18] C.K. Prier, D.A. Rankic, D.W. Macmillan, Chem. Rev. 113 (2013) 5322–5363.
[19] Y. Li, B. Yuan, Z. Sun, W. Zhang, Green Synth. Catal. 2 (2021) 267–274.
[20] G. Sun, M. Zuo, W. Qian, et al., Green Synth. Catal. 2 (2021) 32–37.
[21] Y. Ning, T. Ohwada, F.E. Chen, Green Synth. Catal. 2 (2021) 247–266.
[22] X. Ju, D. Li, W. Li, W. Yu, F. Bian, Adv. Synth. Catal. 354 (2012) 3561–3567.
[23] Z. Liang, S. Xu, W. Tian, R. Zhang, Beilstein J. Org. Chem. 11 (2015) 425–430.
[24] T.P. Nicholls, G.E. Constable, J.C. Robertson, M.G. Gardiner, A.C. Bissember, ACS Catal. 6 (2016) 451–457.
[25] J.T. Guo, D.C. Yang, Z. Guan, Y.H. He, J. Org. Chem. 82 (2017) 1888–1894.
[26] A.K. Yadav, L.D.S. Yadav, Tetrahedron Lett. 58 (2017) 552–555.
[27] X.L. Yang, J.D. Guo, T. Lei, et al., Org. Lett. 20 (2018) 2916–2920.
[28] J. Li, W. Bao, Y. Zhang, Y. Rao, Org. Biomol. Chem. 17 (2019) 8958–8962.
[29] T. Mandal, S. Das, S. De Sarkar, Adv. Synth. Catal. 361 (2019) 3200–3209.
[30] A.M. Ranieri, L.K. Burt, S. Stagni, et al., Organometallics 38 (2019) 1108–1117.
[31] J. Mateos, F. Rigodanza, A. Vega-Peñaloza, et al., Angew. Chem. Int. Ed. 59 (2020) 1302–1312.
[32] G. Perumal, M. Kandasamy, B. Ganesan, et al., Tetrahedron 80 (2021) 131891.
[33] Z.J. Wang, S. Ghasimi, K. Landfester, K.A.I. Zhang, Adv. Synth. Catal. 358 (2016) 2576–2582.
[34] A.P. Côté, A.I. Benin, N.W. Ockwig, et al., Science 310 (2005) 1166–1170.
[35] R. Liu, K.T. Tan, Y. Gong, et al., Chem. Soc. Rev. 50 (2021) 120–242.
[36] K. Geng, T. He, R. Liu, et al., Chem. Rev. 120 (2020) 8814–8933.
[37] P.J. Waller, F. Gándara, O.M. Yaghi, Acc. Chem. Res. 48 (2015) 3053–3063.
[38] P.J. Waller, F. Gándara, O.M. Yaghi, Acc. Chem. Res. 48 (2015) 3053–3063.
[39] X. Feng, X. Ding, D. Jiang, Chem. Soc. Rev. 41 (2012) 6010–6022.
[40] W. Liu, Q. Su, P. Ju, et al., ChemSusChem 10 (2017) 664–669.
[41] Y. Zhi, Z. Li, X. Feng, et al., J. Mater. Chem. A 5 (2017) 22933–22938.
[42] W. Huang, J. Byun, I. Rörich, et al., Angew. Chem. Int. Ed. 57 (2018) 8316–8320.
[43] P.F. Wei, M.Z. Qi, Z.P. Wang, et al., J. Am. Chem. Soc. 140 (2018) 4623–4631.
[44] M. Bhadra, S. Kandambeth, M.K. Sahoo, et al., J. Am. Chem. Soc. 141 (2019) 6152–6156.
[45] R. Chen, J.L. Shi, Y. Ma, et al., Angew. Chem. Int. Ed. 58 (2019) 6430–6434.
[46] W. Hao, D. Chen, Y. Li, et al., Chem. Mater. 31 (2019) 8100–8105.
[47] S. Liu, W. Pan, S. Wu, et al., Green Chem. 21 (2019) 2905–2910.
[48] M. Tian, S. Liu, X. Bu, J. Yu, X. Yang, Chem. Eur. J. 26 (2020) 369–373.
[49] Z. Almansaf, J. Hu, F. Zanca, et al., ACS Appl. Mater. Interfaces 13 (2021) 6349–6358.
[50] Z. Liang, H. Guo, H. Lei, R. Cao, Chin. Chem. Lett. (2021), doi:10.1016/j.cclet.2021.11.055.
[51] G. Jiang, X. Liu, H. Jian, et al., Chin. Chem. Lett. 33 (2022) 3049–3052.
[52] H.K. Li, H.L. Ye, X.X. Zhao, et al., Chin. Chem. Lett. 32 (2021) 2851–2855.
[53] Y. Hou, X. Zhang, J. Sun, et al., Microporous Mesoporous Mater. 214 (2015) 108–114.
[54] S. Lin, C.S. Diercks, Y.B. Zhang, et al., Science 349 (2015) 1208–1213.
[55] N.J. Turro, V. Ramamurthy, J.C. Scaiano, Modern Molecular Photochemistry of Organic Molecules, University Science Books, Sausalito, 2010, p. 252.
[56] W. Huang, Z.J. Wang, B.C. Ma, et al., J. Mater. Chem. A 4 (2016) 7555–7559.
[57] W. Huang, B.C. Ma, H. Lu, et al., ACS Catal. 7 (2017) 5438–5442.
[58] M. Silvi, C. Verrier, Y.P. Rey, L. Buzzetti, P. Melchiorre, Nat. Chem. 9 (2017) 868–873.
[59] H.G. Roth, N.A. Romero, D.A. Nicewicz, Synlett 27 (2016) 714–723.
[60] N.G. Connelly, W.E. Geiger, Chem. Rev. 96 (1996) 877–910.